Pressure and Density Series Equations of State for Steam as Derived from the Haar–Gallagher–Kell Formulation

R. A. Dobbins and K. Mohammed

Brown University, Providence, Rhode Island 02912

D. A. Sullivan

Southeastern Massachusetts University, North Dartmouth, Massachusetts 02747

Received May 8, 1987; revised manuscript received August 17, 1987

Two equations of state for the properties of steam, which are in the form of power series in pressure and density, are developed from the HGK84 formulation. These equations are of high accuracy in the equilibrium region where extensive measurements exist. They also accurately represent the extrapolated data in the metastable region between the vapor saturation and spinodal lines. The accuracy of the representations as a function of the number of terms of the series is presented. Their greatest utility is their use for high accuracy calculations that involve small to moderate departures from ideal-gas behavior. Conversion relationships for the second through the tenth coefficients of the pressure and density series, which apply to the corresponding virial coefficients, are presented. The pressure and density expansions are advantageous for efficient numerical calculations of water vapor properties in the equilibrium and metastable regions.

Key words: steam; virial equation; thermodynamic properties; metastable vapor; spinodal curve; HGK84; IAPS84.

Contents

List of Tables

List of Figures

1. Introduction

The equilibrium thermodynamic properties for water have been recently summarized by an equation of state first

presented as an extended analytic equation,[1] subsequently in tabular form,[2] and finally in a dimensionless formulation.[3] All three of these representations are substantially identical as they are based on the same accumulation of recognized experimental data. Here, we will refer primarily to the second of these[2] which is frequently referred to as HGK84 and which, for scientific and general use, replaces earlier formulations of the properties of steam. For industrial use, the changes in property values may not be significant and the continued use of earlier formulations[4] has been recommended.[5] The new formulation has considerable advantage over its antecedents for certain applications.

An equation of state that is in the form of a power series has a number of advantages in several applications. The power series equation lends itself to efficient numerical calculations which can be executed with far greater speed than is possible with HGK84. Metastable steam vapor is observed in a number of applications of technical interest. Analyses of these processes require pressure–volume–temperature (PVT) information even though direct observations of these properties do not exist. In this case, the power series equations are of special relevance because they facilitate the extrapolation from the extensively measured superheated region into the metastable region.

The justification of the extrapolation into the metastable region of the equations which have been fitted in the equilibrium region is, at best, tentative. Noteworthy experiments have been conducted by Skripov and colleagues[6–8] which show that the density and speed of sound of liquid water and their derivatives are continuous when it passes from an equilibrium state into superheated metastable equilibrium. Comparable experimental information for the metastable water vapor is not available. However, experiments have been conducted with oxygen and nitrogen[10] and, in the instances of these gases, suggests that property values can be extrapolated from the equilibrium region.[11]

A number of experimental studies of the expansion of steam to the point at which supersaturation collapses have been conducted wherein careful measurement of pressure and nozzle area have been observed. In these measurements, the vapor clearly has been expanded to a metastable state well beyond the saturated vapor boundary prior to the onset of condensation. In these studies,[12] the measured pressure profile shows close agreement with theoretical predictions using the earlier IFC equation of state, thereby supporting the derivation of thermodynamic data by extrapolation from this equation of state into the metastable region.

2. Derivation of the Density Series Coefficients

2.1. Virial Equation

The virial equation of state was first used as an empirical equation for fitting PVT data. One of the earliest uses of a truncated form of the virial equation is due to Thiesen.[13] The formal development of the virial equation of state as an infinite series in density is attributed to Kamerlingh Onnes[14]:

$$\text{Pressure } P = RT \sum_{i=1}^{\infty} B_i \rho^i,$$

or

$$\text{Compressibility factor } Z = \frac{P}{\rho RT} = \sum_{i=1}^{\infty} B_i \rho^{i-1}, \quad (1)$$

where P is pressure, T is temperature, ρ is density, and R is the gas constant. $B_1 = 1$ which represents the ideal-gas term in the expansion and functions B_i $(i > 1)$ are the *virial coefficients* which are function of temperature only. Equation (1) is also known as the Leiden series. A similar series expansion can be written in terms of pressure, instead of density:

$$\text{Compressibility factor } Z = \frac{P}{\rho RT} = \sum_{i=1}^{\infty} B'_i P^{i-1}. \quad (2)$$

The pressure series, also known as the Berlin series, is technically not a virial equation and the functions B'_i are not equal to but related to the virial coefficients B_i of (1) by a set of conversion (or inversion) formulas which will be developed later.

Kamerlingh Onnes was careful to refer to the functions $B_i(T)$ as virial coefficients only for the infinite expansion. He noted that if a truncated form of the virial equation is used to fit experimental data, only the lower order resultant functions B_i approximate the "true" virial coefficients. He suggested the name "virial remainder function" for the higher order term to clearly denote that they are not virial coefficients.

Since series expansions which are developed herein are truncated expansions from data of limited accuracy, we cannot correctly call the derived B_i functions virial coefficients. However, the method of determining the B_i functions and the inversion formulas does apply to virial coefficients. Only the lowest order term B_2 contains any valid virial coefficient data.

2.2. HGK84 Equation

HGK84[2] is a complex form of the Helmholtz free-energy equation of state $A(\rho,T)$ which accurately describes thermodynamic properties of fluid water from the dilute vapor to compressed liquid states. Unlike previous equations of state for steam, HGK84 is a single analytic formulation covering the entire fluid state, rather than a collection of equations describing various regions.[4] This provides a higher degree of thermodynamic consistency. This single equation consists of four terms: ideal-gas equation (i), base function (b), residual function (r), and critical region correction function (c).

$$A(\rho,T) = A_i(T) + A_b(\rho,T) + A_r(\rho,T) + A_c(\rho,T). \quad (3)$$

In the following derivation, the critical region correction will be ignored. As will be shown later, this omission precludes accurate agreement between HGK84 and the series expansion near the critical point. The ideal-gas function of Ref. 2 is used directly. The virial coefficients (or B_i functions of a finite polynomial) can be found by first writing the ith density derivative of pressure from Eq. (1):

$$\left(\frac{\partial^{(i)} P}{\partial \rho^{(i)}}\right)_T = (i!)RTB_i + [(i+1)!]RTB_{i+1}\rho + \cdots. \quad (4)$$

The individual virial coefficients are found by taking the limit of the equation above:

$$B_i(T) = [(i!)RT]^{-1} \lim_{\rho \to 0} \left(\frac{\partial^{(i)} P}{\partial \rho^{(i)}} \right)_T \quad (5)$$

The pressure derivatives can be related to the Helmholtz function by $P = \rho^2 \partial A / \partial \rho$.

We see from Eq. (3) that the virial coefficient depends on both the base and residual functions. These components will be denoted by the subscripts b and r:

$$B_i = B_{i,b} + B_{i,r}. \quad (6)$$

The derivation of each component is described in the following sections.

2.3. Base Function

The base function of HGK84 is

$$A_b(\rho,T) = RT\{ -\ln(1-y) - (\beta-1)/(1-y) + (\alpha+\beta+1)/[2(1-y)^2] + 4y(\overline{B}/b - \gamma) - (\alpha-\beta+3)/2 + \ln(\rho RT/P_0)\}, \quad (7)$$

where α, β, γ, and P_0 are constants, $y = b\rho/4$. The two molecular parameters b and $\overline{B}$ are functions of temperature:

$$b = b_1 \ln(T_r) + \sum_{j=0,1,3,5} b_j T_r^{-j}, \quad (8)$$

$$\overline{B} = \sum_{j=0,1,2,4} C_j T_r^{-j}, \quad (9)$$

where T_r is the reduced temperature T/T_0 ($T_0 = 647.03$ K). C_j and b_j are constants.

The base function contribution to the virial coefficients are

$$\begin{aligned} B_{2,b} &= \overline{B}, \\ B_{3,b} &= (b/4)^2[1 - 2(\beta-1) + 3(\alpha+\beta+1)], \\ B_{4,b} &= (b/4)^3[1 - 3(\beta-1) + 6(\alpha+\beta+1)], \\ B_{5,b} &= (b/4)^4[1 - 4(\beta-1) + 10(\alpha+\beta+1)], \\ &\cdots\cdots, \end{aligned} \quad (10)$$

where $\overline{B}$ is the second virial coefficient which has been incorporated into the base function of HGK84. The higher order terms can be generalized for $B_{i,b}$ ($i > 2$) as

$$B_{i,b} = (b/4)^{i-1}[1 - (i-1)(\beta-1) + \left(\sum_{j=1}^{i-1} j\right)(\alpha+\beta+1). \quad (11)$$

2.4. Residual Function

The residual function consists of a 36-term expansion determined by a global, least-squares fit to experimental data.

$$A_r(\rho,T) = \sum_{i=1}^{36} g_i T_r^{-l(i)} (1 - e^{-\rho})^{k(i)}, \quad (12)$$

where g_i, $l(i)$, and $k(i)$ are constants. Defining G_n as

$$G_n = \sum_{i=1}^{36} g_i T_r^{-l(i)} | k(i) = n, \quad (13)$$

we are able to express the residual function contribution to the virial coefficients by

$$\begin{aligned} (0!)RTB_{2,r} &= G_1, \\ (1!)RTB_{3,r} &= -G_1 + G_2, \\ (2!)RTB_{4,r} &= G_1 - 3G_2 + 2G_3, \\ (3!)RTB_{5,r} &= -G_1 + 7G_2 - 12G_3 + 6G_4, \\ (4!)RTB_{6,r} &= G_1 - 15G_2 + 50G_3 - 60G_4 + 24G_5, \\ (5!)RTB_{7,r} &= -G_1 + 31G_2 - 180G_3 + 390G_4 - 360G_5 + 120G_6, \\ (6!)RTB_{8,r} &= G_1 - 63G_2 + 602G_4 - 2100G_4 + 3360G_5 - 2520G_6 + 720G_7, \\ (7!)RTB_{9,r} &= -G_1 + 127G_2 - 1932G_3 + 10\,206G_4 - 25\,300G_5 + 31\,920G_6 - 20\,160G_7 + 5040G_8, \\ (8!)RTB_{10,r} &= G_1 - 255G_2 + 6050G_3 - 46\,620G_4 + 166\,824G_5 - 317\,520G_6 + 332\,640G_7 - 181\,440G_8 + 440\,320G_9. \end{aligned} \quad (14)$$

3. Conversion to Pressure Series

Epstein,[15] in 1952, published an algebraic method for the calculation of pressure-series virial coefficients as functions of the density-series virial coefficients. Epstein's paper also gives the pressure-series relations for the second to fifth virial coefficients (B'_2 to B'_5). A year later, Putnam and Kilpatrick[16] presented a different solution to the same problem and noted an error in Epstein's formula for B'_5. Putnam and Kilpatrick's solution has now been implemented by a computer algorithm and used to develop the conversion formula for the first nine pressure-series virial coefficients. These formulas are given in Table 1. Values for both the density and pressure series coefficients are given in Table 2. The derivation of the density expansion and some of the pressure series conversion formulas have been verified by two investigators.

TABLE 1. Pressure series virial coefficients

$$(RT)^1B' = B$$
$$(RT)^2C' = C - B^2$$
$$(RT)^3D' = D - 3BC + 2B^3$$
$$(RT)^4E' = E - 2C^2 - 4BD + 10B^2C - 5B^4$$
$$(RT)^5F' = F - 5CD - 5BE + 15BC^2 + 15B^2D - 35B^3C + 14B^5$$
$$(RT)^6G' = G - 3D^2 - 6CE + 7C^3 - 6BF + 42BCD + 21B^2E - 84B^2C^2 - 56B^3D + 126B^4C - 42B^6$$
$$(RT)^7H' = H - 7DE - 7CF + 28C^2D - 7BG + 28BD^2 + 56BCE - 84BC^3 + 28B^2F - 252B^2CD - 84B^3E + 420B^3C^2 + 210B^4D - 462B^5C + 132B^7$$
$$(RT)^8I' = I - 4E^2 - 8DF - 8CG + 36CD^2 + 36C^2E - 30C^4 - 8BH + 72BDE + 72BCF - 360BC^2D + 36B^2G - 180B^2D^2 - 360B^2CE + 660B^2C^3 - 120B^3F + 1320B^3CD + 330B^4E - 1980B^4C^2 - 792B^5D + 1716B^6C - 429B^8$$
$$(RT)^9J' = J - 9EF - 9DG + 15D^3 - 9CH + 90CDE + 45C^2F - 165C^3D - 9BI + 45BE^2 + 90BDF + 90BCG - 495BCD^2 - 495BC^2E + 495BC^4 + 45B^2H - 495B^2DE - 495B^2CF + 2970B^2C^2D - 165B^3G + 990B^3D^2 + 1980B^3CE - 4290B^3C^3 + 495B^4F - 6435B^4CD - 1287B^5E + 9009B^5C^2 + 3003B^6D - 6435B^7C + 1430B^9$$

$B = B_2$, $C = B_3$, $D = B_4$, $E = B_5$,...,$J = B_{10}$.

4. Thermodynamic Relations

Thermodynamic properties such as enthalpy, internal energy, and entropy are readily determined from the classical thermodynamic relationships. Each property can be represented as the sum of an ideal gas (i) and real gas or excess ($*$) quantity.

Pressure
$$P = \rho^2 \frac{\partial A}{\partial \rho} = Z\rho RT = RT \sum_{i=1} B_i \rho^i, \tag{15}$$

Internal energy
$$u = A + Ts,$$
$$u = u_i + u_*,$$
$$u_i = \int c_{vi} dT,$$
$$u_* = \int \left(P - T\frac{\partial P}{\partial \rho}\right)\rho^{-2}\, d\rho = -RT^2 \sum_{i=2} \left(\frac{dB_i}{dT}\right)\frac{\rho^{i-1}}{i-1}, \tag{16}$$

Enthalpy
$$h = u + P/\rho = u + ZRT, \tag{17}$$

Isochoric heat capacity
$$c_v = -T\frac{\partial^2 A}{\partial T^2}$$
$$c_v = c_{vi} + c_{v*},$$
$$c_{vi} = c_{vi}(T),$$
$$c_{v*} = -\int T\rho^{-2}\frac{\partial^2 P}{\partial \rho^2}\, d\rho = -RT \sum_{i=2} \left(2\frac{dB}{dT} + T\frac{d^2B}{dT^2}\right)\rho^{i-1}, \tag{18}$$

Isobaric heat capacity
$$c_p = c_v + \frac{T}{\rho^2}\left(\frac{\partial P}{\partial T}\right)^2 \Big/ \left(\frac{\partial P}{\partial \rho}\right), \tag{19}$$

Entropy
$$s = -\left(\frac{\partial A}{\partial T}\right)_\rho$$
$$s = s_i + s_*,$$
$$s_i = \int \frac{c_{pi}}{T}\, dT - R \ln\left(\frac{P}{P_{\text{ref}}}\right),$$
$$s_* = \int \left[R\rho - \frac{\partial P}{\partial T}\right]\frac{d\rho}{\rho^2} = -R \sum_{i=2} \left(B + T\frac{dB}{dT}\right)\frac{\rho^{i-1}}{(i-1)}, \tag{20}$$

Speed of sound
$$c^2 = \left(\frac{c_p}{c_v}\right)\left(\frac{\partial P}{\partial \rho}\right)_T. \tag{21}$$

5. Comparison of Density Expansion to HGK84

The region within the coexistence boundary in the PV plane is divided into three regions: metastable liquid, unstable, and metastable vapor. The unstable region is characterized by the positive slope of the (theoretical) isotherm, $(\partial P/\partial V)_T$ as shown in Fig. 1. Two regions of metastable fluid exist between the unstable reigon and the equilibrium coexistence boundary. The focus of the present investigation is directed toward the estimation of thermodynamic properties in the stable and metastable vapor regions. As noted above, no accurate experimental PVT data for metastable vapor are available. Therefore, our basis for comparison must be the HGK84 equation of state from which the density and pressure series expansion were derived.

TABLE 2. Values of density and pressure series coefficients

Temp. K	300	400	500	600
Density Series Expansion Coefficients				
B_2	-6.2144E-002	-1.9610E-002	-9.5719E-003	-5.6032E-003
B_3	-5.7842E-003	-4.7928E-004	-5.0752E-005	-5.7015E-006
B_4	5.80276E-005	5.04810E-006	7.15806E-007	1.90502E-007
B_5	-1.7577E-007	-1.4188E-008	-2.4975E-009	-1.0493E-009
B_6	7.70390E-012	-7.9138E-012	2.53185E-012	3.60712E-012
B_7	1.43229E-012	1.55473E-013	7.39633E-015	-9.4649E-015
B_8	-5.0440E-015	-5.0946E-016	-3.4114E-017	1.97863E-017
B_9	1.02578E-017	1.00963E-018	7.27149E-020	-3.2775E-020
B_{10}	-1.4540E-020	-1.4142E-021	-1.0465E-022	4.21568E-023
dB_2/dT	9.72370E-004	1.69740E-004	5.79027E-005	2.68441E-005
dB_3/dT	1.57469E-004	1.11295E-005	1.11688E-006	1.23314E-007
dB_4/dT	-1.5773E-006	-1.1110E-007	-1.1951E-008	-1.8897E-009
dB_5/dT	4.96842E-009	3.11055E-010	3.08480E-011	6.62999E-012
dB_6/dT	-1.6763E-012	1.80799E-013	3.99724E-014	-6.7732E-015
dB_7/dT	-3.3444E-014	-3.4787E-015	-4.4674E-016	-1.8673E-017
dB_8/dT	1.23904E-016	1.14431E-017	1.39325E-018	8.64019E-020
dB_9/dT	-2.5592E-019	-2.2760E-020	-2.7121E-021	-1.3329E-022
dB_{10}/dT	3.65184E-022	3.19454E-023	3.76751E-024	2.62900E-025
d^2B_2/dT^2	-2.2315E-005	-2.2407E-006	-5.1389E-007	-1.7994E-007
d^2B_3/dT^2	-4.6432E-006	-2.6950E-007	-2.4776E-008	-2.7191E-009
d^2B_4/dT^2	4.67317E-008	2.67305E-009	2.46471E-010	2.95784E-011
d^2B_5/dT^2	-1.5214E-010	-7.8845E-012	-6.2591E-013	-6.5704E-014
d^2B_6/dT^2	8.74972E-014	-1.2618E-015	-8.9250E-016	-1.8063E-016
d^2B_7/dT^2	8.47723E-016	7.22110E-017	9.56379E-018	1.40914E-018
d^2B_8/dT^2	-3.3221E-018	-2.4787E-019	-2.9856E-020	-4.1739E-021
d^2B_9/dT^2	6.97034E-021	5.00238E-022	5.82913E-023	7.96609E-024
d^2B_{10}/dT^2	-1.0012E-023	-7.0673E-025	-8.1131E-026	-1.0964E-026
Pressure Expansion Coefficients				
B_2'	-4.4883E-007	-1.0623E-007	-4.1480E-008	-2.0234E-008
B_3'	-5.0318E-013	-2.5347E-014	-2.6737E-015	-4.8378E-016
B_4'	-5.6525E-019	-6.0765E-021	-2.0309E-022	-1.2111E-023
B_5'	-9.5406E-025	-2.2903E-027	-2.4233E-029	-6.0597E-031
B_6'	-1.7248E-030	-9.0877E-034	-3.0629E-036	-2.8131E-038
B_7'	-3.3884E-036	-3.9456E-040	-4.2327E-043	-1.5245E-045
B_8'	-6.9528E-042	-1.7853E-046	-6.1023E-050	-8.3616E-053
B_9'	-1.4772E-047	-8.3721E-053	-9.1177E-057	-4.8212E-060
B_{10}'	-3.2189E-053	-4.0255E-059	-1.3972E-063	-2.8334E-067
Saturated Vapor				
P, kPa	3.53570	245.533	2,637.29	12,339.4
d, kg/m^3	0.0255775	1.36792	13.1896	72.8105
Z(HGK84)	0.998407	0.972291	0.866489	0.612009
Z(dens.)*	0.998407	0.972291	0.866489	0.612009
Z(pres.)*	0.998407	0.972291	0.866495	0.618314

* 10 term expansion

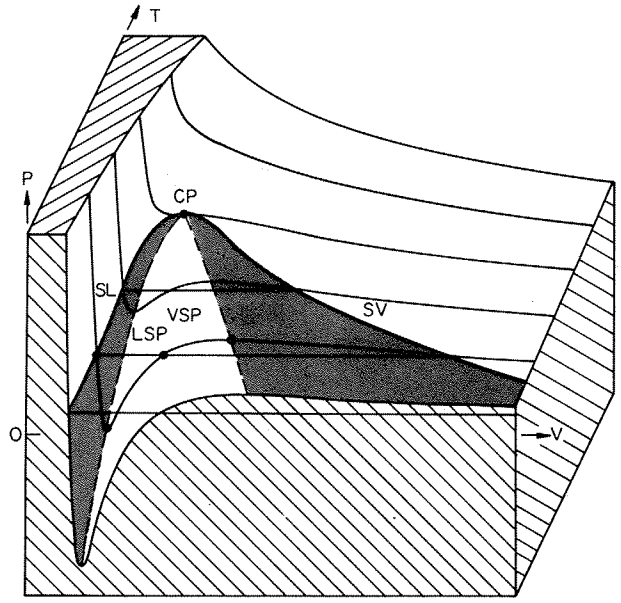

FIG. 1. PVT surface defining the various fluid regions and their boundaries. The shaded regions are metastable state. CP–critical point, SV–saturated vapor, SL–saturated liquid, LSP–liquid spinodal curve, VSP–vapor spinodal curve.

The vapor pressure and vapor-side spinodal curves are shown in Fig. 2 along with a number of isochores. As noted by Skripov,[17] the isochores exhibit considerable curvature close to the spinodal curve and are tangent to it. The increase in isochore curvature is responsible for rapid change in thermodynamic properties near the spinodal curve. Table 3 contains spinodal curve PVT coordinates computed from HGK84.

A comparison of the density expansion using a different number of terms to the HGK84 equation is shown in Figs. 3 and 4 for isotherms of 300, 400, 500, and 600 K. Expansions of four or five terms appear accurate up to (and slightly beyond) the spinodal curve for the 300 and 400 K isotherms. The agreement in the metastable vapor region diminishes at higher temperature. The inclusion of additional terms in the density expansion improves the agreement with HGK84 at the higher temperatures.

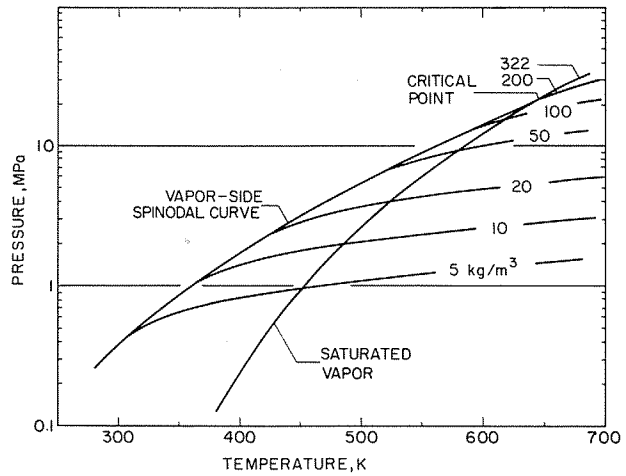

FIG. 2. PT diagram of water showing the saturated vapor and vapor spinodal curves and various isochores.

TABLE 3. Vapor-side spinodal curve based on HGK84

Temperature (K)	Pressure (MPa)	Density (kg/m³)
280.0	0.2606	3.5970
290.0	0.3172	4.2157
300.0	0.3822	4.9041
310.0	0.4566	5.6679
320.0	0.5414	6.5132
330.0	0.6376	7.4467
340.0	0.7462	8.4759
350.0	0.8684	9.6085
360.0	1.0055	10.8533
370.0	1.1589	12.2194
380.0	1.3301	13.7172
390.0	1.5204	15.3574
400.0	1.7317	17.1520
410.0	1.9655	19.1139
420.0	2.2239	21.2573
430.0	2.5086	23.5976
440.0	2.8219	26.1521
450.0	3.1658	28.9396
460.0	3.5426	31.9811
470.0	3.9549	35.3004
480.0	4.4053	38.9243
490.0	4.8965	42.8846
500.0	5.4315	47.2163
510.0	6.0136	51.9623
520.0	6.6464	57.1726
530.0	7.3337	62.9088
540.0	8.0799	69.2443
550.0	8.8900	76.2712
560.0	9.7694	84.1081
570.0	10.7248	92.9067
580.0	11.7636	102.8682
590.0	12.8950	114.2695
600.0	14.1302	127.5098
610.0	15.4836	143.2077
620.0	16.9745	162.4257
630.0	18.6324	187.3618
640.0	20.4826	215.6285
647.1	22.0550	322.0000

The ability of the density expansion to predict the location of the spinodal curve at low temperatures led us to investigate whether such a density expansion is able to predict the spinodal curve in the region approaching the critical point. Using increasing number of terms, we found the spinodal locus by numerical iteration to satisfy the condition $(\partial P/\partial \rho)_T = 0$. These results are shown in Fig. 5. At low temperatures, the spinodal locus occurs at low densities (relative to the critical density). Hence, only a few terms of the expansion are needed to accurately predict the location of the spinodal curve in the PVT plane near the triple point. At higher temperatures (and correspondingly higher densities), additional terms in the expansion are required. Five terms are sufficient for temperatures to 560 K. Since the critical region (adjustment) terms in Helmholtz Eq. (3) have been omitted in the present derivations, agreement in the temperature range of 600 to 647.13 K (the critical temperature) is not possible.

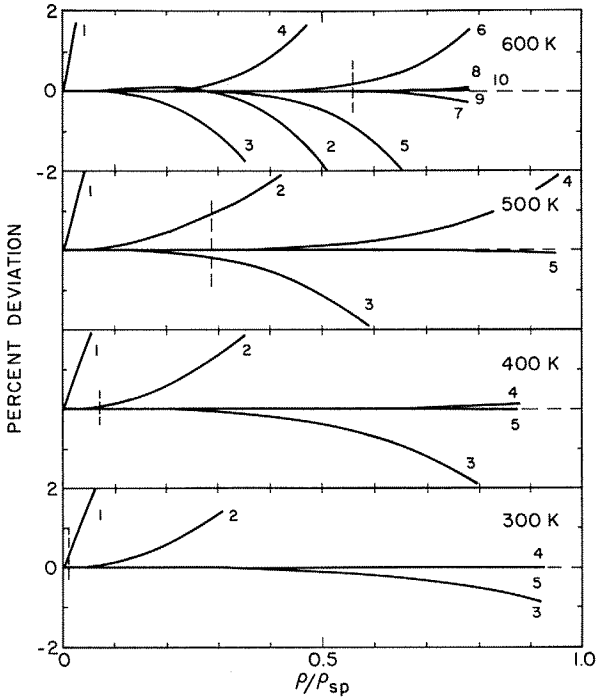

FIG. 3. Deviation in predicting the compressibility factor Z for selected isotherms as a function of the dimensionless density ratio ρ/ρ_{sp}, where ρ_{sp} is the denisty on the vapor spinodal curve. The numbers indicate the number of terms in the density series. The vertical dashed lines indicate saturated vapor.

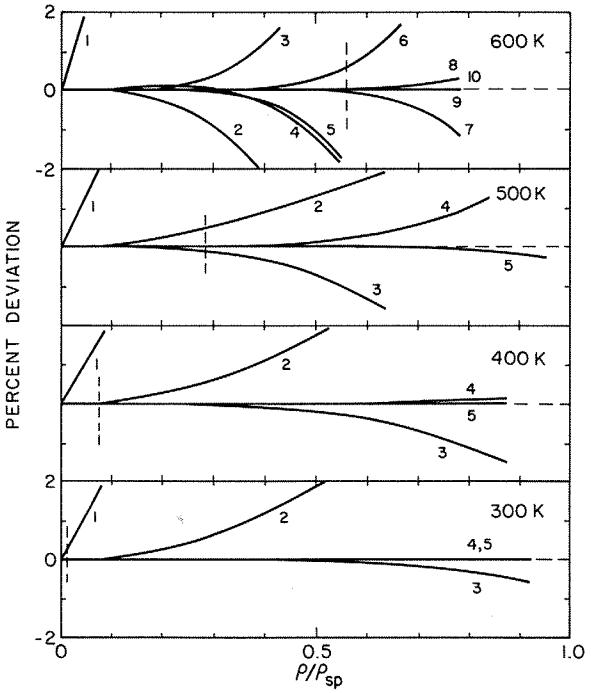

FIG. 4. Deviation in predicting the sound speed c for selected isotherms as a function of the dimensionless density ratio ρ/ρ_{sp}, where ρ_{sp} is the density on the vapor spinodal curve. The numbers indicate the number of terms in the density series. The vertical dashed lines indicate saturated vapor.

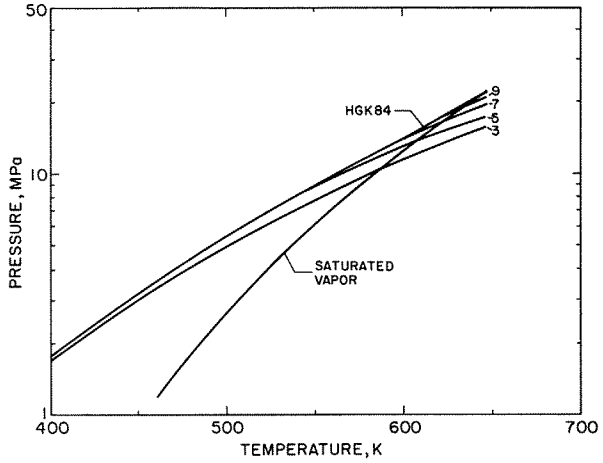

FIG. 5. Density series prediction of the spinodal curve. Numbers indicate the number of terms in the series.

6. Computational Speed and Other Factors

The computational speed of the series expansions has been tested against an optimized version of an HGK84 computer program written in Pascal. To insure a valid basis for comparison, both the optimized HGK84 and density series expansion programs calculated the same set of thermodynamic properties, namely, the compressibility factor, internal energy, enthalpy, isochoric, and isobaric heat capabilities and several derivatives of pressure. Furthermore, both programs were compiled and executed using the same compiler and computer. Both HGK84 and the density series expansion are explicit in temperature and density. A time test using these thermodynamic coordinates showed the density expansion to be faster by a factor of 5.3 for the two-term expansion and 2.2 for the ten-term expansion.

In many practical applications, a high accuracy equation explicit in pressure and temperature is desired which involves only the first several virial coefficients and an estimate of the accuracy that these terms provide. The HGK84 formulation cannot be readily expressed with pressure and temperature as the explicit variables. Hence, the calculation of density as a function of pressure and temperature involves iteration. The pressure series expansion provides a noniterative solution which increases the computational speed relative to HGK84. If, for example, four iterations are required to solve HGK84, then pressure series expansion computation is faster by a factor of 8 to 20.

The rapid solution of an equation by iteration depends on several factors, one of which is the initial estimate of explicit variables. The series expansions presented herein are accurate equations of state by themselves. In addition, they can be used to provide initial estimates of density for the iterative solution of other equations of state, such as HGK84.

In applications involving subcritical steam, it is most often the equilibrium vapor region which is of interest. For a given pressure in this region, the thermodynamic properties along the saturated vapor boundary represent the largest de-

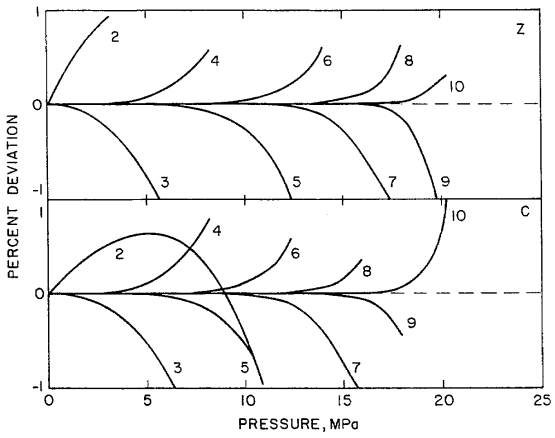

FIG. 6. Deviation in predicting the compressibility factor Z and sound speed c along the saturated vapor boundary. Numbers indicate the number of terms in the density series.

viation from ideal-gas behavior. For the determination of properties for low-pressure steam, a series expansion containing only a few terms can achieve sufficient precision for most applications. For example, in the metering of low-pressure steam by means of an orifice or flow nozzle, the uncertainty in the discharge coefficient of the primary flow element is typically 0.6%. If a sufficient number of terms are included in the series expansion to reduce the deviation between the truncated expansion and the full HGK84 equation to within, say, 0.1% along the saturated vapor boundary, then the systemic bias introduced in the superheated vapor region will be insignificant compared to other sources of errors and uncertainties. Figure 6 indicates that only four terms in the density expansion are required to keep the deviation within 0.1% for pressure 5 MPa, and eight terms for pressures to 15 MPa.

Since the sound speed depends on derivatives of the thermodynamic properties, the magnitude of its derivation is often much larger than that for Z. In some instances, even the general nature of the deviation curves are quite different. One unexpected result of the present investigation is that deviations in sound speed are comparable in magnitude and the deviation curves resemble those for Z. This, perhaps fortuitous, result indicates that polytropic flow processes can be accurately calculated using the present pressure or density series.

7. References

[1]L. Haar, J. S. Gallagher, and G. S. Kell, in *Proceedings of the 8th Symposium on Thermophysical Properties*, edited by J. V. Sengers (ASME, New York, 1982), Vol. II, p. 298.
[2]L. Haar, J. S. Gallagher, and G. S. Kell, *NBS/NRC Steam Tables* (Hemisphere, Washington, DC, 1984).
[3]J. Kestin, J. V. Sengers, and B. Kamgar-Parsi, J. Phys. Chem. Ref. Data **13**, 175 (1984).
[4]C. A. Meyer, R. B. McClintock, G. J. Silvestri, and R. C. Spencer, Jr., *ASME Steam Tables*, 5th ed. (ASME, New York, 1983).
[5]H. J. White, Mech. Eng. **108**, 36 (1986).
[6]V. N. Chukanov and V. P. Skripov, Teplofiz. Vys. Temp. **9**, 739 (1971).
[7]V. N. Evstefeev, V. N. Chukanov, and V. P. Skripov, Teplofiz. Vys. Temp. **15**, 659 (1977).
[8]V. N. Evstefeev, V. N. Chukanov, and V. P. Skripov, Teploenergetika **9**, 66 (1977).
[9]V. N. Evstefeev, V. P. Skripov, and V. N. Chukanov, Teplofiz. Vys. Temp. **17**, 299 (1979).
[10]R. C. Hendricks, R. J. Simoneau, and R. F. Barrows, NASA TN D-8169 (1976).
[11]D. A. Sullivan, and P. A. Thompson, in *Mass Flow Measurements—1984* (ASME, New York, 1984).
[12]J. W. Hedback, "Theorie der Spontanen Kondensation in Duesen und Turbinen," Ph.D. thesis, Institute fur Thermische Turbomaschinen, Eidenoessichen T. H., Zurich, 1982.
[13]M. Thiesen, Ann. Phys. **24**, 467 (1885).
[14]H. K. Onnes, Comm. Phys. Lab. Leiden, Nos. 71 and 74 (1901).
[15]L. F. Epstein, J. Chem. Phys. **20**, 1981 (1952).
[16]W. E. Putnam and J. E. Kilpatrick, J. Chem. Phys. **21**, 951 and 1112 (1953); J. E. Kilpatrick, *ibid.*, 274.
[17]V. P. Skripov, "A Study of Water in Metastable Phase States: The Attained Level and the Problems," International Association for the Properties of Steam Meeting, Duesseldorf, West Germany, September 1986.